EUSIPCO2020
28th European Signal Processing Conference
January 18-22, 2021
Amsterdam

Second-Order Horizontal Synchrosqueezing of the S-transform: a Specific Wavelet Case Study

Dominique Fourer and François Auger

January 20, 2020

ibisc
université evry val-d'essonne
université PARIS-SACLAY
IREENA
Institut de Recherche en Energie Electrique de Nantes Atlantique - EA 4642
UNIVERSITÉ DE NANTES

Purpose of this work

Goals

- Computing efficient representations for handling non-stationary multicomponent signals
- Dealing with impulsive-like and/or strongly amplitude- and frequency-modulated signals
- Reversible representation allowing an extraction of the elementary deterministic signal components
- Link with the wavelet theory extending our previous work on the time-reassigned synchrosqueezed STFT [Fourer,Auger,2019]

$\Rightarrow$ **Proposed approach:** Time-frequency analysis combined with reassignment-based post-processing methods to improve the readability

Context: the French ANR ASCETE project (ANR-19-CE48-0001): 2019-2023

ASCETE: Analysis and Separation of Complex Signal: Exploiting the Time-Frequency Structure

PROJET FINANCÉ PAR L'ANR - PROJECT FUNDED BY THE ANR

Project holder: Dr. Sylvain Meignen (LJK, Grenoble, France)

Goals:

- Extends to previous methods (developed in ASTRES project)
- Combines deterministic signal processing methods with stochastic models
- New applications to audio, biomedicine, astrophysics, etc.

https://www-ljk.imag.fr/ASCETE/

Content

1. Introduction
2. Time-Reassigned Synchrosqueezed S-transform
   - Reassignment and synchrosqueezing
   - Second-order time-reassigned synchrosqueezed S-transform
3. Numerical Results
   - Time-frequency representations
   - Signal reconstruction
4. Conclusion

The S-transform [Stockwell et al., 1996]

Generalization of the Short-Time Fourier Transform (STFT) using a frequency-dependent analysis window.

Definition

The S-transform of a zero-mean signal x is defined for a central frequency $\omega_0 > 0$ at any time t and radial frequency ω as:

$$\mathrm{ST}_x^h(t,\omega) = \frac{|\omega|}{\omega_0} \int_{-\infty}^{+\infty} x(\tau) h\left(\frac{\omega}{\omega_0}(t-\tau)\right)^* \mathbf{e}^{-j\omega\tau}\, d\tau \tag{1}$$

with $j^2 = -1$ and z^* the complex conjugate of z.

h is chosen as a Gaussian window with time-spread parameter T:
$h(t) = g(t, T) = \frac{1}{\sqrt{2\pi}T}\, \mathbf{e}^{-\frac{t^2}{2T^2}}$,
which leads us to:

$$\mathrm{ST}_x^g(t,\omega) = \frac{|\omega|}{\omega_0} \int_{-\infty}^{+\infty} x(\tau) g\left(\frac{|\omega|}{\omega_0}(t-\tau), T\right)^* \mathbf{e}^{-j\omega\tau}\, d\tau \tag{2}$$

$$= \mathbf{e}^{-j\omega t} \int_{-\infty}^{+\infty} x(t+\tau) g\left(-\tau, \frac{\omega_0 T}{|\omega|}\right)^* \mathbf{e}^{-j\omega\tau}\, d\tau \tag{3}$$

Link with the Continuous Wavelet Transform (CWT)

The CWT of a signal x at each time t and scale s for an admissible mother wavelet Ψ (*i.e.* satisfying $C_\Psi = \int_{\mathbb{R}} |F_\Psi(\omega)|^2 \frac{d\omega}{|\omega|} < +\infty$, with $F_x(\omega) = \int_{-\infty}^{+\infty} x(t)\,\mathbf{e}^{-j\omega t} dt$) is:

$$W_x(t,s) = \frac{1}{\sqrt{|s|}} \int_{-\infty}^{+\infty} x(\tau)\Psi\left(\frac{\tau - t}{s}\right)^* d\tau \tag{4}$$

If we define $s = \frac{\omega_0}{\omega}$, Eq. (4) can be expressed as as:

$$\mathrm{CW}_x(t,\omega) = \sqrt{\frac{|\omega|}{\omega_0}} \int_{-\infty}^{+\infty} x(\tau)\Psi\left(\frac{\omega}{\omega_0}(\tau - t)\right)^* d\tau. \tag{5}$$

The Morlet mother wavelet $\Psi(t) = \frac{\pi^{-1/4}}{\sqrt{T}}\,\mathbf{e}^{\frac{-t^2}{2T^2}}\,\mathbf{e}^{j\omega_0 t}$ leads to:

$$\mathrm{MW}_x(t,\omega) = \sqrt{\frac{|\omega|}{\omega_0 T\sqrt{\pi}}} \int_{-\infty}^{+\infty} x(\tau)\,\mathbf{e}^{-\frac{\omega^2(t-\tau)^2}{2(\omega_0 T)^2}}\,\mathbf{e}^{-j\omega(\tau - t)}\,d\tau \tag{6}$$

$$= \sqrt{\frac{2\sqrt{\pi}\omega_0 T}{|\omega|}}\,\mathbf{e}^{j\omega t}\mathrm{ST}_x^g(t,\omega) \tag{7}$$

The S-transform can be viewed as a specific (rescaled) continuous wavelet transform

$$\mathrm{ST}_x^g(t,\omega) = \sqrt{\frac{|\omega|}{2\sqrt{\pi}\omega_0 T}}\,\mathbf{e}^{-j\omega t}\,\mathrm{MW}_x(t,\omega) \tag{8}$$

S-transform marginalization and inversion formula 1/2

Using the frequency domain expression of the S-transform

$$\mathrm{ST}_x(t,\omega) = \int_{-\infty}^{+\infty} F_x(\Omega+\omega) F_h\left(\frac{\omega_0}{\omega}\Omega\right) \mathbf{e}^{j\Omega t} \frac{d\Omega}{2\pi}$$

Marginalization with respect to frequency

$$\int_{-\infty}^{+\infty} \mathrm{ST}_x(t,\omega)\,\mathbf{e}^{j\omega t} \frac{d\omega}{|\omega|} = \iint_{\mathbb{R}^2} F_x(\omega+\Omega) F_h\left(\frac{\omega_0}{\omega}\Omega\right) \mathbf{e}^{j(\omega+\Omega)t} \frac{d\Omega}{2\pi} \frac{d\omega}{|\omega|} \quad (9)$$

$$= \iint_{\mathbb{R}^2} F_x(\Omega')\,\mathbf{e}^{j\Omega' t} F_h(\xi-\omega_0) \left(\frac{|\omega_0\Omega'|}{\xi^2} \frac{|\xi|}{|\omega_0\Omega'|}\right) \frac{d\Omega'}{2\pi} d\xi \quad (10)$$

$$= \int_{-\infty}^{+\infty} F_x(\Omega')\,\mathbf{e}^{j\Omega' t} \frac{d\Omega'}{2\pi} \cdot \int_{-\infty}^{+\infty} F_h(\xi-\omega_0) \frac{d\xi}{|\xi|} \quad (11)$$

$$= x(t) \cdot C_h(\omega_0 T) \quad (12)$$

x can be recovered from ST_x using the synthesis formula

$$\boxed{x(t) = \frac{1}{C_h(\omega_0 T)} \int_{-\infty}^{+\infty} \mathrm{ST}_x(t,\omega)\,\mathbf{e}^{j\omega t} \frac{d\omega}{|\omega|}} \quad (13)$$

with $C_h(\omega_0 T) = \int_{-\infty}^{+\infty} \mathbf{e}^{-\frac{(x-\omega_0 T)^2}{2}} \frac{dx}{|x|}$.

S-transform marginalization and inversion formula 2/2

Marginalization with respect to time

$$\int_{-\infty}^{+\infty} \mathrm{ST}_x^g(t,\omega)\, dt = \iint_{\mathbb{R}^2} F_x(\omega+\Omega) F_h\left(\frac{\omega_0}{\omega}\Omega\right)^* \mathbf{e}^{j\Omega t}\, \frac{d\Omega}{2\pi} dt \tag{14}$$

$$= \int_{\mathbb{R}} F_x(\omega+\Omega) F_h\left(\frac{\omega_0}{\omega}\Omega\right)^* \delta(\Omega)\, d\Omega \tag{15}$$

$$= F_x(\omega) F_h(0)^* \tag{16}$$

Eq.(16) is equal to $F_x(\omega)$ when a Gaussian window is used (*i.e.* $F_h(0)=1$).

Hence, x can finally be reconstructed by applying the inverse Fourier transform which leads us to:

$$\boxed{x(t) = \frac{1}{2\pi} \iint_{\mathbb{R}^2} \mathrm{ST}_x^g(\tau,\omega)\, \mathbf{e}^{j\omega t}\, d\tau d\omega} \tag{17}$$

Time-Frequency Representations comparison

Comparison of the TFRs provided by S-transform, the STFT, and the Morlet CWT, applied to the Livingston GW150914 signal [Fourer et al., 2017].

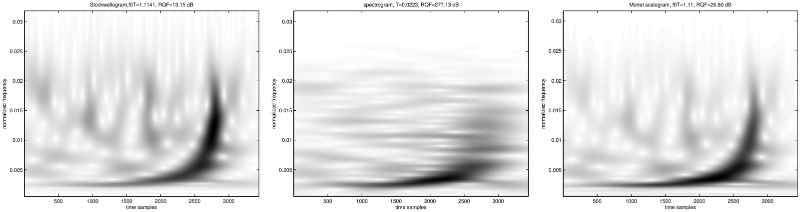

(a) Stockwellogram (b) Spectrogram (c) Scalogram

Reassignment method [Kodera et al., 1978] [Auger & Flandrin 1995]

Principle

Improving the energy concentration (readability) of any bilinear distribution by reassigning its energy to new locations closer to real signal support.
Consider the TFR of a signal x expressed in terms of the Wigner-Ville distribution as:

$$\mathrm{TFR}_x(t,\omega) = \iint_{\mathbb{R}^2} \mathrm{WV}_x(\tau,\Omega)\Phi(t-\tau,\omega-\Omega)d\tau d\Omega$$

Method description

- Computation of the reassignment operators:

$$\hat{t}(t,\omega) = \frac{\int_{\mathbb{R}^2} \tau \mathrm{WV}_x(\tau,\Omega)\Phi(t-\tau,\omega-\Omega)d\tau d\Omega}{\int_{\mathbb{R}^2} \mathrm{WV}_x(\tau,\Omega)\Phi(t-\tau,\omega-\Omega)d\tau d\Omega} \quad (18)$$

$$\hat{\omega}(t,\omega) = \frac{\int_{\mathbb{R}^2} \Omega \mathrm{WV}_x(\tau,\Omega)\Phi(t-\tau,\omega-\Omega)d\tau d\Omega}{\int_{\mathbb{R}^2} \mathrm{WV}_x(\tau,\Omega)\Phi(t-\tau,\omega-\Omega)d\tau d\Omega}. \quad (19)$$

- **Computation of the reassigned time-frequency representation**:

$$\mathrm{RTFR}_x(t,\omega) = \int_{\mathbb{R}^2} \mathrm{TFR}_x(\tau,\Omega)\delta(t-\hat{t}(\tau,\Omega))\delta(\omega-\hat{\omega}(\tau,\Omega))\, d\tau d\Omega \quad (20)$$

The resulting reassigned TFR is a sharpened but non-reversible TFR, due to the loss of the phase information.

The reassigned Stockwellogram

Reassignment operators

The reassignment operators can be reworded using S-transforms with modified analysis window (cf. [Fourer, Auger, hal-01467244, 2015] for the detailed proof):

$$\tilde{t}_x(t,\omega) = t - \frac{\mathrm{ST}_x^{\mathcal{T}g}(t,\omega)}{\mathrm{ST}_x^{g}(t,\omega)}, \qquad \tilde{\omega}_x(t,\omega) = j\omega + \frac{\mathrm{ST}_x^{\mathcal{D}g}(t,\omega)}{\mathrm{ST}_x^{g}(t,\omega)}, \tag{21}$$

$$\hat{t}_x(t,\omega) = \mathrm{Re}(\tilde{t}_x(t,\omega)), \qquad \hat{\omega}_x(t,\omega) = \mathrm{Im}(\tilde{\omega}_x(t,\omega)) \tag{22}$$

with $\mathcal{T}g(t) = tg(t)$ and $\mathcal{D}g(t) = \frac{dg}{dt}(t)$.

Reassignment

The reassigned Stockwellogram is finally computed as:

$$\mathrm{R}_x(t,\omega) = \iint_{\mathbb{R}^2} |\mathrm{ST}_x^g(\tau,\Omega)|^2 \, \delta\left(t - \hat{t}_x(\tau,\Omega)\right) \delta\left(\omega - \hat{\omega}_x(\tau,\Omega)\right) d\tau \, d\Omega. \tag{23}$$

Synchrosqueezing [Daubechies and Maes, 1996, 2011] [Thakur 2011]

Principle

- A particular reassignment method which allows to compute sharpen and reversible TFRs by moving the transform instead of its energy.
- Allows mode extraction by a ridge detection and local region integration procedure.

Synchrosqueezed S-transform (frequency-reassigned) [Fourer, Auger et al. 2015]

Based on the marginalization respect to frequency given by Eq. (12).

- Synchrosqueezed S-transform:

$$\mathrm{SST}_x(t,\omega) = |\omega| \int_{\mathbb{R}} \mathrm{ST}_x(t,\omega')\, \mathbf{e}^{j\omega' t} \delta\left(\omega - \hat{\omega}(t,\omega')\right) \frac{\mathrm{d}\omega'}{|\omega'|}, \tag{24}$$

- Reconstruction formula:

$$\hat{x}(t) = \frac{1}{C_h(\omega_0 T)} \int_{\mathbb{R}} \mathrm{SST}_x(t,\omega) \frac{\mathrm{d}\omega}{|\omega|}, \tag{25}$$

Time-reassigned S-transform

Principle

- A new S-transform synchrosqueezing method based on the marginalization with respect to time given by Eq. (16).
- Inprovement of the readability of impulsive and strongly frequency-modulated component using an enhanced group-delay estimator.

Time-reassigned Synchrosqueezed S-transform

$$S_x^g(t,\omega) = \int_{\mathbb{R}} \mathrm{ST}_x^g(\tau,\omega)\, \delta\left(t - \hat{t}_x(\tau,\omega)\right) d\tau. \tag{26}$$

Signal Reconstruction

$$\int_{\mathbb{R}} S_x^g(t,\omega) dt = \iint_{\mathbb{R}^2} \mathrm{ST}_x^g(\tau,\omega)\delta\left(t - \hat{t}_x(\tau,\omega)\right) d\tau dt \tag{27}$$

$$= \int_{\mathbb{R}} \mathrm{ST}_x^g(\tau,\omega) d\tau = F_x(\omega) \tag{28}$$

Hence, we obtain the exact reconstruction formula:

$$\boxed{\hat{x}(t) = \iint_{\mathbb{R}^2} S_x^g(\tau,\omega)\, \mathbf{e}^{j\omega t}\, d\tau \frac{d\omega}{2\pi}} \tag{29}$$

An enhanced Second-Order group-delay estimator 1/2

AM/FM signal model

$$x(t) = \mathbf{e}^{\lambda_x(t)+j\phi_x(t)} \tag{30}$$

$$\text{with} \quad \lambda_x(t) = l_x + \mu_x t + \nu_x \frac{t^2}{2} \tag{31}$$

$$\text{and} \quad \phi_x(t) = \varphi_x + \omega_x t + \alpha_x \frac{t^2}{2} \tag{32}$$

where $\lambda_x(t)$ and $\phi_x(t)$ are respectively the log-amplitude and the phase. This signal verifies $\frac{dx}{dt}(t) = (q_x t + p_x)x(t)$ with $q_x = \nu_x + j\alpha_x$, $p_x = \mu_x + j\omega_x$.

Properties

Differentiating with respect to t when $|\mathrm{ST}_x^g(t,\omega)| > 0$, allows to compute:
$\frac{\partial \mathrm{ST}_x^g}{\partial t}(t,\omega) = \mathrm{ST}_x^{\mathcal{D}g}(t,\omega) = -j\omega \mathrm{ST}_x^g(t,\omega) + (p_x + q_x t)\mathrm{ST}_x^g(t,\omega) - q_x \mathrm{ST}_x^{\mathcal{T}g}(t,\omega)$

$$\text{Hence,} \quad \frac{\mathrm{ST}_x^{\mathcal{D}g}(t,\omega)}{\mathrm{ST}_x^g(t,\omega)} = p_x - j\omega + q_x \left(t - \frac{\mathrm{ST}_x^{\mathcal{T}g}(t,\omega)}{\mathrm{ST}_x^g(t,\omega)} \right) \tag{33}$$

and finally: $\boxed{\tilde{\omega}_x(t,\omega) = p_x + q_x \tilde{t}_x(t,\omega)}$

An enhanced Second-Order group-delay estimator 2/2

$$t_x^{(2)} = \frac{\omega - \omega_x}{\alpha_x} = \hat{t}_{x(t,\omega)} + \frac{\omega - \hat{\omega}_{x(t,\omega)}}{\alpha_x} + \frac{\nu_x}{\alpha_x}\mathrm{Im}(\tilde{t}_{x(t,\omega)}) \qquad (34)$$

which can be estimated by:

$$\boxed{\hat{t}_x^{(2)}{}_{(t,\omega)} = \begin{cases} \frac{\omega - \hat{\omega}_x(t,\omega) + \mathrm{Im}(\hat{q}_x(t,\omega)\,\tilde{t}_x(t,\omega))}{\mathrm{Im}(\hat{q}_x(t,\omega))} & \text{if } \mathrm{Im}(\hat{q}_{x(t,\omega)}) \neq 0 \\ \hat{t}_x(t,\omega) & \text{otherwise} \end{cases}} \qquad (35)$$

where $\hat{q}_{x(t,\omega)}$ can be computed as [Fourer, Auger et al., 2015]:

$$\hat{q}_x(t,\omega) = \frac{(\mathrm{ST}_x^{\mathcal{D}g}(t,\omega))^2 - \mathrm{ST}_x^{\mathcal{D}^2 g}(t,\omega)\mathrm{ST}_x^{g}(t,\omega)}{\mathrm{ST}_x^{\mathcal{T}\mathcal{D}g}(t,\omega)\mathrm{ST}_x^{g}(t,\omega) - \mathrm{ST}_x^{\mathcal{T}g}(t,\omega)\mathrm{ST}_x^{\mathcal{D}g}(t,\omega)} \qquad (36)$$

with $\mathcal{D}^2 g(t,T) = \frac{d^2 g}{dt}(t,T)$ and $\mathcal{T}\mathcal{D}g(t,T) = t\frac{dg}{dt}(t,T)$.

Second-order horizontal synchrosqueezed S-transform

Principle

Consists in moving $\mathrm{ST}_x^g(t,\omega)$ from the point (t,ω) to the point $(t_x^{(2)},\omega)$ such that $\frac{d\phi_x}{dt}(t_x^{(2)}) = \omega_x + \alpha_x t_x^{(2)} = \omega$.

Second-order horizontal synchrosqueezed S-transform is obtained by replacing $\hat{t}_x$ by the second-order enhanced group-delay estimator $\hat{t}_x^{(2)}$.

Second-order horizontal synchrosqueezed S-transform

$$S_x^{g(2)}(t,\omega) = \int_{\mathbb{R}} \mathrm{ST}_x^g(\tau,\omega)\, \delta\left(t - \hat{t}_x^{(2)}(\tau,\omega)\right) d\tau. \tag{37}$$

Signal Reconstruction

The same reconstruction formula used by the (first-order) time-reassigned synchrosqueezed S-transform:

$$\boxed{\hat{x}(t) = \iint_{\mathbb{R}^2} S_x^{g(2)}(\tau,\omega)\, \mathbf{e}^{j\omega t}\, d\tau \frac{d\omega}{2\pi}} \tag{38}$$

Implementation consideration

Discretization

Computations are based on the rectangular approximation method and a uniform sampling approximation:
$\mathrm{ST}_x^g[k,m] \approx \mathrm{ST}_x^g(\frac{k}{F_s}, 2\pi\frac{mF_s}{M})$, F_s being the sampling frequency.
$k \in \mathbb{Z}$ is the time sample index and $m \in \mathcal{M}$ is the discrete frequency bin.
M is chosen as an even number: $\mathcal{M} = [-M/2+1; -1] \cup [1; M/2]$.

Gaussian window approximation

A threshold Γ is applied to obtain a finite number of time samples K_m at each time frame, when $\mathbf{e}^{-\frac{m^2(K_m/2)^2}{2(f_0T)^2M^2}} \leq \Gamma$:

$$K_m \geq \frac{2Mf_0T\sqrt{2\log(1/\Gamma)}}{|m|}. \tag{39}$$

with $\omega_0 = 2\pi f_0$.
In practice, we used $\Gamma = 10^{-4}$ which provides good results with a reasonable computation time.

TFRs comparison (RE=Rényi Entropy at order $\alpha = 3$)

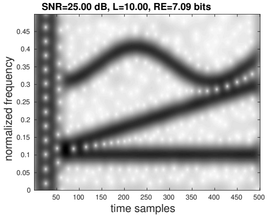

(d) spectrogram

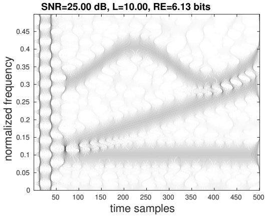

(e) time-reassigned synchrosqueezed STFT

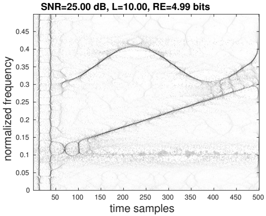

(f) second-order horizontal synchrosqueezed STFT

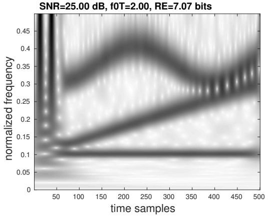

(g) stockwellogram

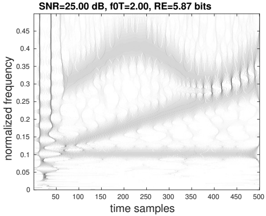

(h) time-reassigned synchrosqueezed S-transform

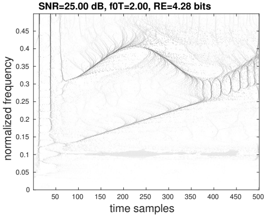

(i) second-order horizontal synchrosqueezed S-transform

Signal reconstruction quality comparison

Reconstruction quality factor

$$\mathrm{RQF}(x, \hat{x}) = 10 \log_{10} \left(\frac{\sum_k |x[k]|^2}{\sum_k |x[k] - \hat{x}[k]|^2} \right), \quad (40)$$

Table : Reconstruction quality of the S-transform, the first- and the second-order horizontal synchrosqueezed S-transforms with $f_0 T = 2$, M varying from 300 to 2000 (a) and Γ varying from 10^{-1} to 10^{-4} (b).

(a)	M ($\Gamma = 10^{-4}$)	300	500	1000	2000
	RQF (dB)	0.85	54.10	60.12	66.14
(b)	Γ ($M = 500$)	10^{-1}	10^{-2}	10^{-3}	10^{-4}
	RQF (dB)	53.45	54.10	54.10	54.10

Contributions summary

Summary

- A new second-order horizontal synchrosqueezing method based on an enhanced group-delay estimator designed for the S-transform
- Efficient computation using an S-transform with specific analysis windows
- A preliminary comparative evaluation of the S-transform with the STFT-based second-order horizontal synchrosqueezing

Future work

- Consideration of new signal models (e.g. hyperbolic chirp, high-order polynomial phase, etc.)
- Real-world application scenarios involving signal components extraction

Matlab code freely available at: `https://fourer.fr/sthsst/`